Topological Changes of Hydrogen Bonding of Water with Acetic Acid: AIM and NBO Studies

Vasiliy S. Znamenskiy and Michael E. Green*

Department of Chemistry, City College of the City University of New York, New York, New York 10031

Received: March 12, 2004; In Final Form: June 1, 2004

Hydrogen bonding has been studied in a model system, originally devised for the KcsA K^+ ion channel, using density functional calculations. The model was to represent the putative gating region of the channel. Four acetic acids here are fixed at approximately 4-fold symmetry; six water molecules are added. Initial configurations had two water molecules in the center of the near-square defined by the carboxyls of the acetic acids, plus one water at each corner on the outside. Certain configurations of the acetic acids allow an extra water molecule to move into the center of the group; a move of 0.1 Å by the acetic acids suffices to produce this jump (>2 Å). In certain cases, the inner and outer water positions were nearly isoenergetic. Atoms in molecules (AIM) and natural bond orbital (NBO) provide complementary techniques for studying the changes in bonding and in electron density that accompany the different positions of the water molecules, including discontinuous changes in the topology of bonding. Two principle conclusions result: (1) All hydrogen bonds in this system belong to a single continuum with respect to their AIM and bonding properties, over the range of strength and length of bonds, irrespective of whether the oxygen is a water oxygen or bonded to a carbon in a carboxyl group. (2) Trajectories in molecular dynamics simulations are unlikely to sample such discontinuities correctly; this is likely to apply to systems other than that modeled here.

Introduction

This work continues our earlier studies on hydrogen bonds that switch between short, strong hydrogen bonds (SSHB) and normal hydrogen bonds.[1,2] A study by Grabowski[3] used AIM (atoms in molecules[4−6]) to study a particular set of hydrogen bonds, leading him to propose a single parameter for hydrogen bond strength of a range of hydrogen bonds. In the latter of our earlier two studies, AIM showed a case of switching between partially covalent and purely noncovalent hydrogen bonding. NBO (natural bond orbitals[7]) was also used to study the nature of the bonding, in what turned out to be a complementary technique. Since then, a study by Dupre,[8] also using both AIM and NBO, has considered a different system, getting information somewhat similar to what our earlier work had found. Mallinson and co-workers have used these techniques to understand hydrogen bonding in ionic complexes of 1,8-bis(dimethylamino)naphthalene;[9] here, crystal structures were available from which to work. Bartlett et al., for example, have discussed the importance of hydrogen bonding with water motion in enzyme catalysis.[10] Earlier, Lin and co-workers[11] discussed properties of hydrogen bonds in a system complex enough to produce bent bonds, with distorted electron distributions. There is a huge literature on hydrogen bonds, partly in relation to proton transfer, and many simulations that include hydrogen bonded systems (essentially all the simulations of biological systems). A number of papers using DFT methods to understand hydrogen bonding in particular systems have also appeared in recent years.[12−15] There is also a large literature on QM/MM (quantum mechanical/molecular mechanical) studies of hydrogen bonded systems, including such methods as MS-EVB,[16−21] and the work of Hammes-Schiffer and co-workers,[22−24] as well as an extensive review of proton-transfer methods by Krasnoholovets and co-workers.[25] Our approach is somewhat different in that it concentrates on local bonding and the electron density and its gradient and Laplacian, treated from the AIM viewpoint. From this we hope to be able to understand what it is that produces transitions in type of hydrogen bonding. In standard MD (i.e., not QM/MM) simulations, the hydrogen bonding is parametrized in such a way as to make such transitions not appear in the calculation. However, there is good evidence that transitions to SSHB or low barrier hydrogen bonds (LBHB) exist and are important (the definitions of these types of bonds may not always be perfectly precise, as we discuss later; in this paper we subsume LBHB under the SSHB heading). The mechanism of enzyme action often leads to changes in hydrogen bond length. One example is tyrosine phosphatase. Simulations indicate reduction in hydrogen bond length up to 0.1 Å going from reactant to transition state, while experimental results on the vanadate analogue showed average reductions of 0.12−0.18 Å.[26] We are not looking at metals, but the phenomenon does not appear to require metals.

The existence of SSHB and LBHB, and their importance in enzymatic reactions, has been discussed by a number of workers, including Frey, Cleland, Lin, and others.[27−32] These are bonds with a short O−O distance, with fairly symmetrical bond lengths between the intermediate hydrogen and the donor and acceptor, or even a single well with essentially no barrier at all between positions of the proton separating donor and acceptor. We are attempting in this work, as we were in the two previous papers, to understand at a fundamental level the conditions affecting the length and strength of hydrogen bonds. For this, it is necessary to consider the effects of surrounding groups, especially as they affect local electron density. We have earlier found that moving the surrounding groups an extremely small distance (≤0.1 Å, sometimes much less), past a transition point, forces a major hydrogen bonding rearrangement. The surround-

* Corresponding author. E-mail: green@sci.ccny.cuny.edu.

10.1021/jp048887z CCC: $27.50
Published on Web 07/14/2004

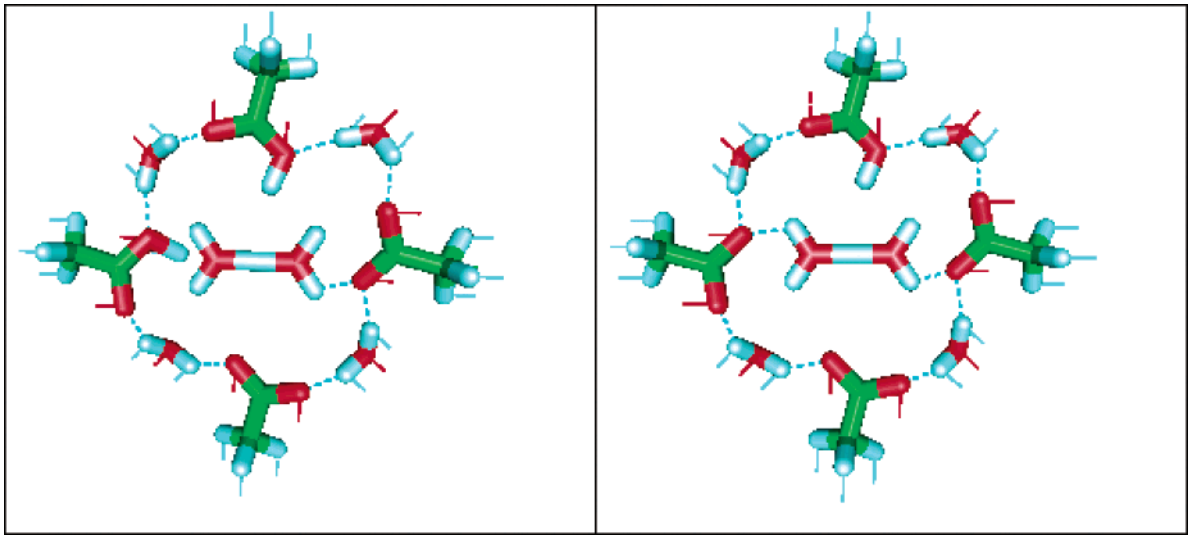

Figure 1. Diagram of the starting positions of the atoms with charge −1 (left panel) and −2 (right panel), using gOpenMol[39] as software. The four acetic acid moieties are shown at the sides; in the center there is an H_5O_2, and there is a water molecule between each pair of acetic acids on the outside. Oxygen atoms are red, hydrogen atoms white, and carbon atoms green. The streaks from each atom show the (forward) direction in which the initial positions were moved for successive optimizations; the initial positions of the H_5O_2 were the same in all cases. Initial hydrogen bonds were added by gOpenMol, using O−O and O−H distances and O−H−O angles as criteria (dotted lines).

ing groups we have studied so far are acetic acids,[1] and chloride ions.[2] In these systems, we have found a switch between SSHB and normal hydrogen bonds with a change of position of surrounding groups of <0.01 Å, at least in the Cl^- case. We have also studied the effect of differing charge on the total system; adding an H^+ can also greatly change the bonding, something that is not a surprise. The fact that the KcsA K^+ channel[33] gates in response to a drop in pH suggested the importance of the change in charge. The original motivation for the studies concerned this gating phenomenon; we have proposed that voltage gated channels also gate with a proton move that changes charge. In this work, however, the gating question is not the main point.[34,35] In all the cases we are interested in, the contraction in hydrogen bond donor−acceptor distance (here, oxygen − oxygen distance in an O−H−O bond) can be over 0.2 Å, from over 2.7 to around 2.5 Å; the latter is in the range usually called an SSHB. While short hydrogen bonds are well-known, the kinds of jumps we see here do not appear to have been studied. We now find that there is a continuum of the hydrogen bonds in our system; while much more work is needed to prove this, we would not be surprised to find that this phenomenon is general. We have not attempted to verify that all Popelier's AIM-based criteria for hydrogen bonds[5] are met by all the bonds we are calling hydrogen bonds, although we are using AIM. However, the fact that essentially all the properties lie on continuous curves with standard hydrogen bonds suggests that we are justified in calling these hydrogen bonds; the first criterion, the existence of a bond critical point, is always fulfilled.

There are few, or probably zero, direct experimental tests known for systems that show complex jumps in their hydrogen bonding topology; because these systems are necessarily fairly large and thus complex, it is to be expected that conventional interpretations of data will be attempted first. One case where it appears likely that effects of the sort we are discussing here are dominant is in the bacterial porin OmpF, where extremely sharp changes in response to pH are found.[36,37] This is reasonable because a change in charge can also produce the type of rearrangement we are discussing. In proteins, catalytic sites are generally near ionizable residues.[10] This is as would be expected if the catalytic conformational changes were hydrogen bond related, although of course it does not constitute proof that they are.

To fully understand the cause of such changes, it is necessary to find the electron density changes that are responsible for it. We also must interpret the electron density in terms that make chemical sense; hence the need for bond orbital studies, as well as for the critical points in electron density, and the Laplacian of the electron density, as given by AIM. We will also be interested in the effective forces exerted by the hydrogen bonding system on the surrounding groups, as these are relevant to the conformational changes that may be induced in the surrounding system as the hydrogen bonds shift. To the extent that ion channel gating involves a conformational change, it should be similar to other protein conformational changes. The relevance to this question, as well as others that involve enzymes, may be found from the interaction of the hydrogen bonding with the surrounding groups. We will look at the critical points of the electron density distribution, defined (as in AIM) as the maxima of the electron density distribution, or the saddle points, or the minima. Complementary information on hydrogen bonding can be obtained by looking at bond orbitals associated with hydrogen using NBO.

Methods

The software used for optimization was Gaussian 03[38] and, for AIM, the version from Biegler-Konig.[6]

Systems were prepared with four acetic acid moieties, either ionized or uncharged, with two water molecules, to start, as H_5O_2 (i.e., with an extra H) in the center of the group. Four other water molecules were arranged outside the near-square formed by the oxygens of the acetic acid groups, as in Figure 1.

There were in total three series of starting configurations used; in one ("forward"), the H_5O_2 in the center was always symmetric, with 2.4 Å O−O distance, and the acetic acids were stepped *away* from the central H_5O_2. The second one ("reverse") was prepared on the way back from the final configuration of the first series (the acetic acids were stepped closer together)

following eq 1, below; third, the new initial positions of the water were created from the optimized positions of the water with the acetic acids frozen at each of the previous two positions.

After one step of optimization going "forward", the four acetic acids were moved to a new position, and the procedure repeated. Going forward, the outside waters were, like the acetic acids, moved 0.1 Å outward in initial position, while the central H_5O_2 was kept the same. All six waters were optimized, while the acetic acids were kept frozen. This was continued for a total of 11 positions, all but one pair with acetic acid position extended by 0.1 Å; the exception was a pair of 0.05 Å steps in the set with −1 charge (thereby producing a 12th configuration). After the initial set was completed, the reverse series was created with the water starting positions moved back toward the previous positions by following eq 1:

$$R^{(i)}_{n+1} = R_n + (R_n - R_{n-1}) = 2R_n - R_{n-1} \qquad (1)$$

where the $R^{(i)}$ are the initial positions of the water molecules on step $n + 1$, and the R positions on the right are the optimized positions at the previous two steps. The waters were reoptimized with the acetic acids fixed, and the new water starting positions set according to eq 1. This procedure revealed a new set of local minima.

Optimizations, using Gaussian03, were done on the waters and ionizable hydrogens of the acetic acids, with the remainder of the acetic acids (ionized or not) fixed. Natural bond orbital (NBO)[7] and atoms in molecules (AIM)[6] calculations were run on the optimized configurations. From this, the energy, critical points of the electron density, the bonding, and other properties were obtained.

Although some preliminary optimizations were done at low level, all final results reported here were carried out using the B3LYP density functional method,[40,41] with the triple-ζ basis set 6-311G**;[42] some have been reoptimized with the 6-311+G** basis set, which adds diffuse functions to all atoms except hydrogen. The optimizations are presented as determined with 6-311G**; however, the energy values, as well as AIM and NBO results (including those in the figures), were redetermined as single point calculations with 6-311+G** in the positions from the 6-311G** optimizations. When the systems were reoptimized as well, the change in position of the waters with the bigger basis set was never more than 0.24 Å in the worst case (biggest move by any water molecule over four checked configurations). The change in interatomic distance for distances less than 2 Å were <0.06 Å. This is the maximum shift of any atom in any reoptimization, and almost all changes were appreciably smaller. The differences in energy were much smaller between neighboring pairs of states (those in which the acetic acids have been moved just 0.1 Å), the absolute value of the difference of 6-311G** pairs does not exceed 0.001H if compared with 6-311+G** pairs. Comparing the two basis sets for four cases in which we have done the full calculation, the larger 6-311+G** is consistently 0.007 to 0.008 H below the 6-311G** energies. Even 0.001 H is about equal to k_BT (k_B = Boltzmann's constant; T = temperature, kelvin; H = hartree); more accurate calculations are too expensive for a complete set at the moment. However, based on the cases we have, we do not have any reason to expect that the conclusions presented in this paper could be affected. If the energy were not redetermined with the 6-311+G** in place of 6-311G** (i.e., 6-311G** optimization/6-311G** energy) it would have been approximately 0.1 H higher for the system. The 6-311G** optimization/6-311+G** energy calculation pair is optimum for combining adequate accuracy with reasonable efficiency, of the cases we tried.

The Berny algorithm was used in the optimizations.

Graphics (Figures 3−7) and curve fitting were carried out using Origin 6.0 from Microcal.

Global Minimum. We do not prove that the lowest minimum we find is the true global minimum (although we have no reason to doubt that it is, we did not do a frequency calculation). Therefore, where a calculated minimum is what is intended, we will refer to *lowest minimum found*, reserving the words *global minimum* for discussion of the true global minimum.

Results

(A) As before,[1,2] we have found that the hydrogen bonding of a system changes drastically with a change in charge or a small change in position of the groups that define the system. The hydrogen bond lengths change on the order of 0.2 Å at certain values of the spacing of the acetic acids that constitute the surrounding groups; that is, these groups surround two or three water molecules. Additional water molecules are on the outside of these groups. These jumps in hydrogen bond lengths are comparable to our previous results. In this work, we have found additionally that water molecules will undergo significant translations, on the order of 2 Å, with a change of ≤0.1 Å in position of the surrounding groups. The energy also goes through a maximum as the transition point is approached, and falls to a minimum on either side. Presumably there should be a potential energy surface that allows for conformational changes, with minima on either side of a ridge that includes one or more saddle points. The system can, in effect, "react", by crossing such a ridge to a new conformation, in which the topology of the hydrogen bonds has rearranged.

(B) Parts A and B of Figure 2 show the positions of the water molecules with total charge −2, as optimized, for conditions before and after one such transition, in which the change in position of the water molecules is evident.

After the series has been completed, new starting configurations were chosen in accordance with eq 1, starting from the final configuration of the initial trajectory, and extrapolating the positions backward. These were optimized in the same manner, and produced a different set of minima. At the 0.7 Å position of the acetic acids (same as the configuration of Figure 2A, before the jump, but with different water starting positions), the system optimized to a different configuration, of lower energy, with the water that had jumped in still in the middle; Figure 2C looks much more like the configuration *after* the jump on the left. The preceding step, Figure 2D, created by extrapolation from the two preceding configurations rather than by moving acetic acids directly back as in parts A and B, looks like Figure 2A with the acetic acids in the Figure 2B position (but there are considerable differences in detail, as can be seen from the bond paths). The combination shows the hysteresis that accompanies the existence of two minima.

When the initial positions of the water molecules are retraced as described by eq 1, the water molecules optimize (using the standard Gaussian criteria for optimization) to a different set of minima than for the "forward" cases. In Figure 3, going forward, we get the circles shown at 0.8 and 0.9 Å, going back the squares at 0.6, 0.5, and 0.3 Å. We have the energy for each minimum point in Figure 3, showing both paths for both starting configurations.

With −1 charge the minima actually cross, and the lowest minimum found switches from one set to the other. This may

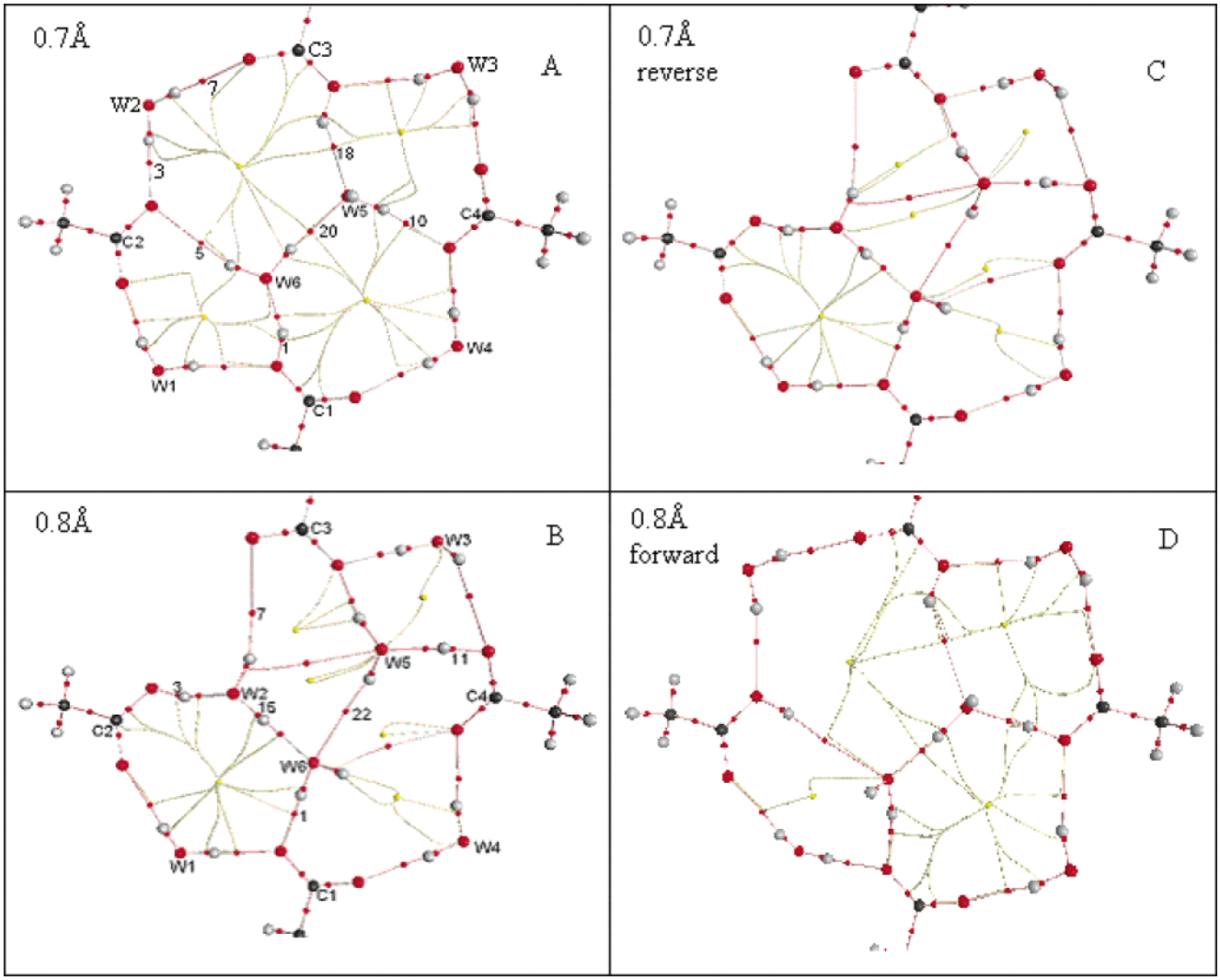

Figure 2. Atomic positions and critical points, shown as two forward AIM molecular graphs (A,B), for the −2 charge case going forward, and one in reverse (C) (per eq 1). In addition, an eq 1 type extrapolation, but in the forward direction, using the 0.6 and 0.7 Å optimized positions for the water initial positions, led to D. This has the same acetic acid positions as B, but the optimized water positions resemble A. Initial positions in A and B were not from an extrapolation; the outer water molecules and acetic acids were placed approximately symmetrically to start, without reference to previous optimizations. The 8th (A) and 9th (B) cases are shown (0.7, 0.8 Å from the first position), where a transition occurs. Large red spheres are oxygen, black carbon, gray hydrogen. Small red spheres are BCP, yellow spheres in the center of rings are RCP, red paths are bond paths, and yellow-gray paths connect BCP to RCP. Waters are labeled W1 − W6 on their oxygens, acetic acids C1 − C4, with the methyl groups on C1 and C3 truncated in the figure. For the −2 charge case, only one major conformational change occurs, at about 0.7 Å. The major jump can be seen by comparing the upper left corners of Figures 2A and 2B, as water W2 moves in. Note the severe changes in bond paths for the other waters. The initial configuration of the water molecules had an approximately symmetrical position for the H_5O_2 in the center. For positions with 0.0 to 0.6 Å, the figures look very much like the 0.7 Å figure; after the major change shown here, the final steps show some change, but not a major change.

in fact happen with −2 charge at distances greater than 1.0 Å forward, but this point was not tested. In other words, different starting positions can optimize to different minima, with standard convergence criteria for Gaussian. Gaussian attempts to find the global minimum, so that this result suggests that there are potential energy basins around structurally significantly different minima; these minima are well enough defined as to prevent further search for a new minimum. The difference in energy between the paths is large, in each case exceeding, at some points, $10k_BT$. At many points the differences are smaller, but even 2- or $3k_BT$ is enough to make a serious difference; if these potentials were used, e.g., for an MD simulation, very different paths would be found, depending on the basin a trajectory began in. It is worth noting that the *energy* of the lowest minimum found for −1 charge remains fairly flat, but the minimum switches from one to the other configuration. Either configuration, at either charge, if taken separately, varies by about 20 k_BT over the range of acetic acid positions, while the lowest minimum found varies, for −1 at least, by only about 7 k_BT. This suggests that the system would be very likely to switch configurations. The behavior on return is really different. With both charges, a water molecule, once it has jumped inside the group of acetic acid residues, does not jump out when the acetic acids return, in the range of coordinates we have studied. This does not make it the true global minimum; the energy is lower with the water outside for some acetic acid positions. An attempt was made to find a third minimum, starting from H_5O_2 set symmetrically within the acetic acid square. However, the symmetric H_5O_2 initial positions in the center converge to one of the other two configurations, with one exception close to one of the minima. This suggests that, with the one exception, there may be only two significant minima. However, not every

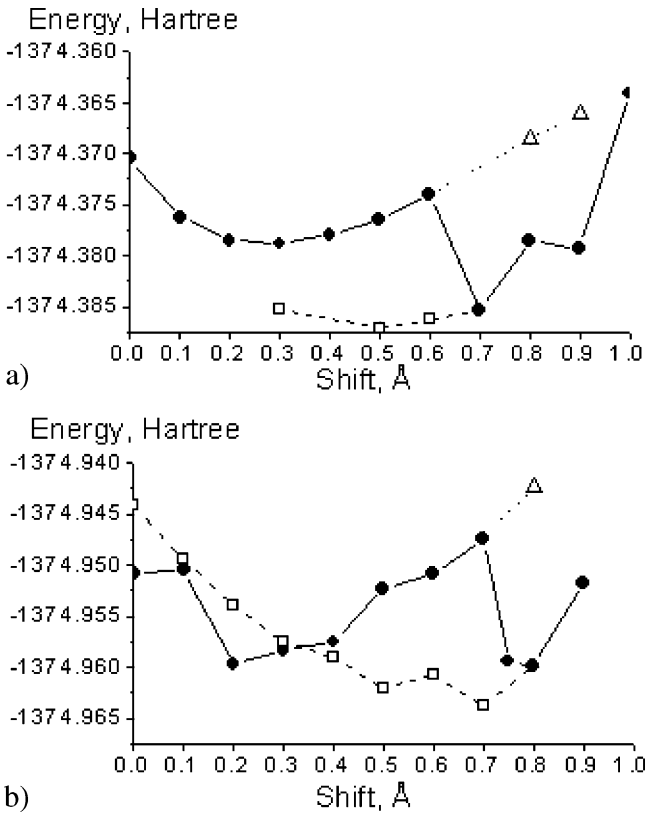

Figure 3. Energy as a function of position: (a) The energy of the system with −2 charge for initial configurations chosen in three different ways; two are those of Figure 2A and 2B, and the third, for the circles at 0.8 and 0.9 Å, from an eq 1 type extrapolation, but in the forward direction. There is no triangle at 0.7 Å because that value did not converge, so the extrapolation is done with 0.2 Å. The solid line shows the results for the initial conditions described in Figure 2. The circles show "forward" initial conditions as just described, and the squares are points obtained by "reverse" extrapolation according to eq 1. At 0.3, 0.5, 0.6, 0.8, and 0.9 Å, there are two separate minima to which the system converged, for different initial positions of the water. (b) The same as a) for charge −1; here the minima cross. There is an additional "forward" point at 0.75 Å, and only one extrapolated point in the forward direction, but a complete set in the "reverse" direction. Two transitions occur, between 0.1 and 0.2 Å, and between 0.75 and 0.8 Å, in the forward direction. Each is accompanied by a drop in energy.

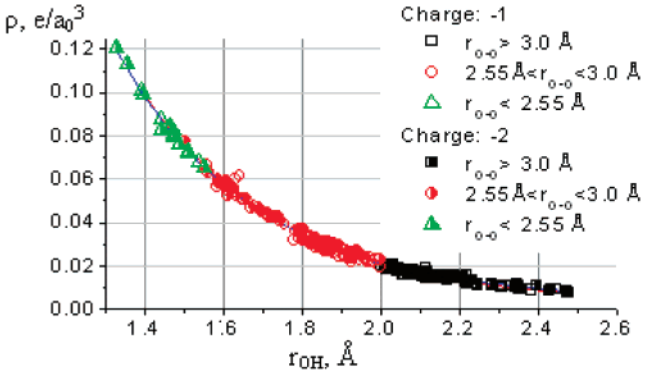

Figure 4. For each O−H BCP in all cases (both charges), combined, the electron density at the BCP is plotted against the O−H distance. Observe that all points fall quite accurately on a single exponential. The curves are fit separately for charge = −1 (red curve) and charge = − 2 (blue curve). Exponential fit to $\rho = \rho_o + A \exp(-r/C)$, with ρ = density at BCP, r = O−H distance: −1 charge, $\rho_o = 0.0028 \pm 0.0007$, $A = 4.7 \pm 0.4$, $C = 0.359 \pm 0.009$; −2 charge, $\rho_o = 0.0038 \pm 0.0006$, $A = 4.8 \pm 0.3$, $C = 0.356 \pm 0.006$. The differences are small enough that the parameters agree within fitting error.

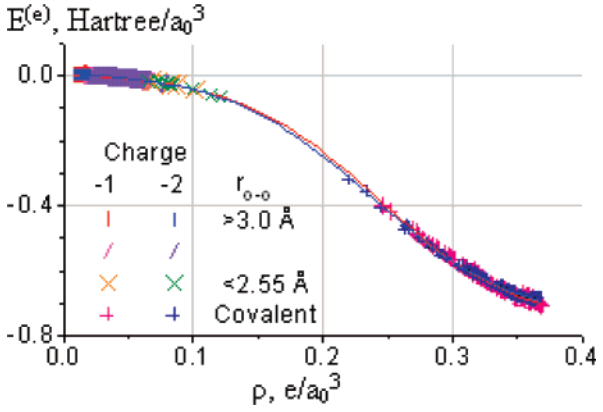

Figure 5. The energy density $E^{(e)}$ = G + V (see Table 1 for some cases) as a function of electron density at the BCP. All O−H bonds are included in this figure; those on the left, near $E^{(e)} = 0$, are hydrogen bonds, those on the right covalent. For all bonds of the systems with a given charge there is a sigmoidal fit: $E = (E_1 - E_2)/(1+\exp((\rho+\rho_o)/P) + E_2$, as shown: −1 charge (red), $E_1 = 0.016 \pm 0.001$, $E_2 = -0.779 \pm 0.003$, $\rho_o = 0.2430 \pm 0.0005$, $P = 0.0557 \pm 0.0007$; −2 charge (blue) $E_1 = 0.018 \pm 0.001$, $E_2 = -0.762 \pm 0.002$, $\rho_o = 0.2369 \pm 0.0005$, $P = 0.0555 \pm 0.0007$. The differences are small enough for the parameters to almost agree within fitting error.

possible case has been tried, so this statement must be regarded as not yet conclusive.

A more detailed analysis of the hydrogen bonds in terms of the electron density and length shows the existence of a range of behavior of the bonds. We will consider this in the next section.

(B) Atoms in molecules (AIM) is a technique for studying the paths followed by the electron density between atoms within a molecule, and it can be applied as well in looking at hydrogen bonds. AIM allows us to study the bonding properties of the system, to observe the switches in bonding and to see whether the bonds are covalent or ionic, among other properties.

We observe from the AIM results that moving the acetic acid molecules 0.1 Å always results in a change of the plot of *bond paths* in some part of the system. Bond paths in AIM are defined as paths of electron density maxima in two dimensions, such that the electron density is higher on the path than on any neighboring line connecting the same two nuclei; furthermore, the molecule must be in a local energy minimum, or the path is not in fact a bond path. In the third dimension, along the path, the electron density decreases away from the bonded nuclei; the minimum along the path is called a *bond critical point* (*BCP*). However, some changes lead to very large changes in bonding over a large fraction of the system, which are reflected in these paths, as well as in the positions of the BCPs. Figure 2 shows the atomic positions, but also shows two molecular graphs, one just before, one after, the jump, with charge −2. The figures show the critical points and bond paths for these two cases. AIM was used to produce similar graphs for all the other configurations. We are investigating the changes in bonding that herald, and that accompany, these changes. For one thing, we find (Figure 4) that there is a relation between the electron density at a hydrogen bond BCP and the length of the bond.

All types of hydrogen bonds, from very strong to very weak, fit on or very near the same curve, which is essentially continuous, and exponential. The exponential dependence is presumably a consequence of the behavior of wave functions at a distance over about 1 Å from the nucleus. Note that all the

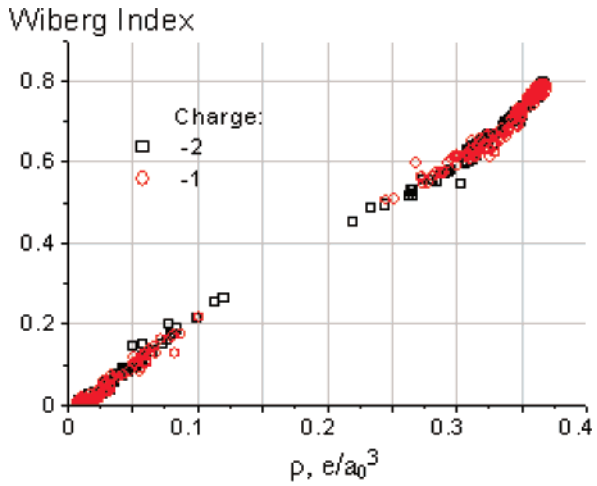

Figure 6. Wiberg bond orbital as found from the Natural Bond Orbital program,[7] as a function of electron density at BCPs. There is an obvious relation between bond order and electron density; those points with high bond order and high electron density correspond to covalent bonds. There is a range of hydrogen bonds, down to very low values of both ρ and bond order, but it remains close to linear. Both charges are included on a single graph.

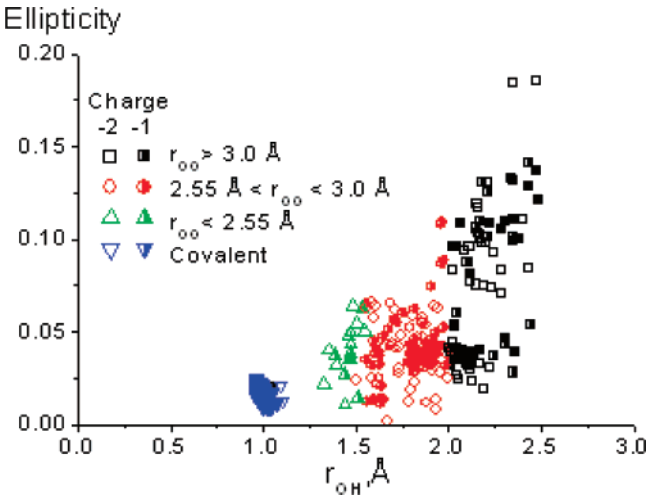

Figure 7. Ellipticity (see text for definition) of BCPs as a function of O − H distance: it is clear that there is a distinction in the average ellipticity as a function of the distance, with weaker bonds, closer to breaking, having generally higher ellipticity. Again, all O−H bonds, from both charges, appear to belong to the same distribution. Tables 2−5 give numerical values for a subset of the bonds. Both charges are shown, and the hydrogen bonds are separated into three groups. The ordinary covalent bonds all have small ellipticity, and practically superimpose. The partially covalent (relatively strong) hydrogen bonds (green triangles) also show fairly low ellipticity; the scatter increases with other hydrogen bonds, especially as they weaken, and approach breaking. "Normal" hydrogen bonds are red circles, weak bonds are black squares.

points still fall on the line even after the transition to a different conformation has been made. An oxygen may form a bond with the same hydrogen, or a different one. It may be long or short. However, the same exponential curve of electron density vs bond length still contains the bond. Therefore, the SSHB and the normal hydrogen bond are not qualitatively different, except that, as shown below, there is some covalent character in the shorter bonds.

While the hydrogen bonds appear to belong to a single population, albeit with somewhat different characteristics at opposite ends of the distribution, there are clearly two very

TABLE 1: Bond Lengths (Å) and AIM Parameters

charge	shift, Å	O−O dist	short O−H dist	long O−H dist	local charge density, some BCP[a] (e/a_o^3)	$E^{(e)}$ of some BCP[a] (hartree/a_o^3)
−2	0	2.59	1.00	1.59	0.0602	−0.011683
−2	0.1	2.85	0.97	2.11	0.0179	0.002008
−2	0.2	2.78	0.98	1.67	0.0298	0.001 11
−2	0.3	2.81	0.97	1.90	0.0279	0.001479
−2	0.4	2.86	0.97	1.97	0.0243	0.001818
−2	0.5	2.92	0.97	2.00	0.0226	0.001839
−2	0.6	2.95	0.97	2.00	0.0226	0.001796
−2	0.9	2.63	1.01	1.62	0.0562	−0.009814
−2	1.0	2.52	1.04	1.49	0.0764	−0.022248
−1	0	2.51	1.05	1.46	0.0826	−0.027201
−1	0.1	2.51	1.04	1.47	0.0807	−0.025694
−1	0.2	2.6	1.01	1.60	0.0579	−0.010321
−1	0.3	2.65	1.00	1.65	0.0505	−0.006559
−1	0.4	2.68	1.00	1.68	0.0475	−0.005235
−1	0.5	2.72	1.00	1.72	0.0424	−0.003043
−1	0.6	2.71	1.00	1.71	0.0434	−0.003579
−1	0.7	2.75	0.99	1.75	0.0394	−0.002046
−1	0.8	2.52	1.02	1.55	0.0651	−0.014700
−1	0.9	2.46	1.05	1.44	0.0874	−0.030755

[a] Some BCP = those involving oxygen atoms of the two central water molecules.

distinct configurations as a function of acetic acid position for the overall system for total charge −2, three configurations for total charge −1. In addition, there are two energy minima, with different hydrogen bond topology, that can be found by Gaussian for most of the acetic acid conformations.

Table 1 shows the fundamental AIM parameters for the BCP of some of the most important hydrogen bonds.

Values of $E^{(e)} = G + V$ (kinetic plus potential energy density) > 0 indicate a noncovalent bond. If $E^{(e)} < 0$ (i.e., $|V| > G$), but $|V| < 2$ G, then the bond is considered to be partially covalent.[43]

We see two characteristics of these plots: first they can each be fitted by a single sigmoidal curve covering not only the hydrogen bonds but the ordinary covalent O−H bonds as well, although the plots are divided into two distinguishable sections, one covering hydrogen bonds, the other the covalent bonds. Second, some of the $E^{(e)}$ values for hydrogen bonds are <0, showing covalent character; there is a continuum, not a sharp distinction, between the two types of bonding, according to this index also. It is already known that energy density and ρ are related for hydrogen bonds, and ρ is therefore sometimes used as a measure of hydrogen bond strength.[44] For each BCP in Table 1, the kinetic and potential energy density, the ellipticity, and the Laplacian of the density, are given. L ($-^1/_4\nabla^2\rho$) gives the local charge concentration, such that a negative L (positive $\nabla^2\rho$) implies that charge is locally depleted, while a positive L means locally concentrated ρ. The topology of L is different from that of the density itself, and does have a set of critical points (not shown). As might be expected, L is also related to the kinetic energy density of the electron.

The types of critical points are related by the Poincare−Hopf relation (in which the four types of CPs—nuclear, bond, ring, and cage—are designated by their initial letters):

$$n - b + r - c = -1 \qquad (2)$$

We found with four Cl^- ions as surrounding groups[2] that this relation was not perfectly satisfied by the critical points of that somewhat similar system. Here we see that it is satisfied, without going beyond the default values given by the AIM software[6] in evaluating these points.

(C) We have also looked at the natural bond orbital (NBO) approach to analyzing this system. Here, the principal quantity

TABLE 2: Ellipticity of Breaking OH Bonds[a]

Charge: −1

		shift									
no.	bond	0	0.1 Å	0.2 Å	0.3 Å	0.4 Å	0.5 Å	0.6 Å	0.7 Å	0.8 Å	0.9 Å
1	$O_{C1}-H_{10}$			0.05	0.05	0.04	0.05	0.04	0.04		
2	$O_{C1}-H_{11}$	0.06	0.07								
3	$O_{C2}-H_{11}$			0.05	0.04	0.04	0.04	0.04	0.04	0.06	0.07
4	$O_{C2}-H_{5}$	0.05	0.12								
5	$O_{C4}-H_{12}$	0.1	0.1	0.13	0.14	0.11	0.12	0.1	0.1	0.06	0.06
6	$O_{W1}-H_{13}$	0.06	0.07							0.03	0.06
7	$O_{W3}-H_{14}$	**0.51**	**0.68**	**0.67**	***0.8***	***1.26***	***2.99***				
8	$O_{W4}-H_{5}$									0.05	0.04
9	$O_{W6}-H_{13}$			0.02	0.03	0.04	0.05	0.07	0.1		
10	$O_{W6}-H_{10}$									0.02	0.02

Charge: −2

		shift										
no.	bond	0	0.1 Å	0.2 Å	0.3 Å	0.4 Å	0.5 Å	0.6 Å	0.7 Å	0.8 Å	0.9 Å	1.0 Å
1	$^{1}O_{C1}-H_{1}$	0.01	0.01	0.01	0.01	0.01	0.01	0.01	0.04	0.04	0.11	
2	$^{2}O_{C1}-H_{2}$											0.03
3	$^{1}O_{C2}-H_{3}$	0.06	0.05	0.05	0.03	0.03	0.03	0.03	0.01	0.01		0
4	$^{1}O_{C2}-H_{4}$										0.06	
5	$^{1}O_{C2}-H_{5}$	0.03		**0.45**	**0.23**	0.18	0.19	**0.21**				
6	$^{2}O_{C2}-H_{5}$		0.04	0.08	**0.26**	**0.52**	***1.38***					
7	$O_{C3}-H_{4}$	0.04	0.04	0.04	0.04	0.04	0.03	0.03	0.13			0.12
8	$^{1}O_{C4}-H_{6}$									***0.93***		
9	$^{1}O_{C4}-H_{7}$										0.04	0.02
10	$^{1}O_{C4}-H_{2}$	0.02	0.03	0.03	0.02	0.01	0.01	0.01				
11	$^{2}O_{C4}-H_{7}$								0.01	0.02		
12	$O_{W1}-H_{5}$										0.02	
13	$O_{W1}-H_{1}$											0.04
14	$O_{W2}-H_{8}$										0.07	
15	$O_{W2}-H_{5}$								0.02	0.02		0.04
16	$O_{W3}-H_{9}$	***0.82***	***1.12***	***1.64***								
17	$O_{W4}-H_{2}$										0.05	
18	$O_{W5}-H_{8}$	0.04	0.04	0.04	0.05	0.05	0.05	0.05	0.02	0.06		
19	$O_{W5}-H_{4}$									**0.25**		
20	$O_{W5}-H_{6}$	0.02	0.13	0.03	0.03	0.05	0.04	0.03			0.02	0.06
21	$O_{W6}-H_{3}$										0.03	
22	$O_{W6}-H_{2}$								0.04	0.07		

[a] Labels on oxygen atoms for charge −2 can be understood from the left panels of Figure 2. Note particularly shifts associated with W2, C2, and C3. The hydrogen atoms in these bonds are those to which these oxygens are bonded. Numbers in italics: $0.8 \leq$ ellipticity. Boldface numbers: $0.2 <$ ellipticity < 0.8. For other parts of the table, the same values are shown as italic or boldface, still based on the ellipticity criteria.

of interest is the bond order between two oxygens and the hydrogen joining them in a hydrogen bond plus a covalent bond, or else in a relatively symmetric pair of hydrogen bonds that may have some covalent character. Short bonds are more symmetric as well as stronger. NBO shows how the bond order varies with distance, whether transitions that appear in the geometry are reflected in the bond orders, and whether it is possible to see a relation between the bond order and the electron density contours. Figure 6 shows how the Wiberg bond orders (given by the NBO 5.0[7] program operating on Gaussian results) correlate with the electron density ρ at the BCPs between hydrogen bonded species. A single curve that can be fit by one straight line covers all hydrogen bonds, at all separations of acetic acids, and both charges. Covalent bonds are in the upper right of the figure, and almost look like an extrapolation of the hydrogen bonds, although that curve is not quite linear. Again we see that the O−H bonds behave as though a single curve, governing their strength and length, describes the entire spectrum of bonds. (Choice of bond order other than that given by the Wiberg partition is possible, but the results do not differ greatly, and it is most important for our purposes to have a consistent set, which this does provide.) Combining this with the known relation between ρ and energy density, as in Figure 5, and the NBO result becomes tied to other properties of hydrogen bonds.

(D) Ellipticity is defined in terms of the ratio of the first two eigenvalues, λ_1 and λ_2, of the Hessian of the density. Specifically, the ellipticity is[5]

$$\epsilon = \lambda_1/\lambda_2 - 1 \tag{3}$$

When the electron density is nearly symmetric about the critical point, $\lambda_1 \approx \lambda_2$, the ellipticity, ϵ, essentially vanishes. In practice, we find very few values larger than 1; the bonding tends to change before the ellipticity becomes any larger. The corresponding electron density contours are elongated. As the ellipticity becomes large, the system approaches a bifurcation point,[5] in which the atoms bond to different partners, and one expects a conformational change, as shown, for example in Figure 2. However, we observe that individual bonds are not informative from this point of view. Tables 2−5 show many of the bonds that exist over only a part of the range of distances.

In some cases, the ellipticity shows that the bonds are clearly stretched ($\epsilon > 0.2$), and they grow, sometimes to $\epsilon > 1$, then disappear. However, some are simply normal bonds that disappear in the course of a conformational change of the entire system.

Tables 2−5 contain a summary of some of the most interesting changes. Note that certain bonds that do not disappear on one side of the transition can shift dramatically in value, by

TABLE 3: Energy Density (Total) of Breaking OH Bonds[a]

Charge = −1, $E^{(e)} \times 10^3$ (hartree/a_o^3)

		shift									
no.	bond	0	0.1 Å	0.2 Å	0.3 Å	0.4 Å	0.5 Å	0.6 Å	0.7 Å	0.8 Å	0.9 Å
1	$O_{C1}-H_{10}$			1.6	1.5	1.2	1.4	0.4	1.2		
2	$O_{C1}-H_{11}$	1.2	2.2								
3	$O_{C2}-H_{11}$			1.4	1.5	2.2	1.4	2.7	1.9	1.6	1.9
4	$O_{C2}-H_5$	0.8	0.7								
5	$O_{C4}-H_{12}$	2.7	2.7	1.1	1.0	1.5	1.0	2.3	1.4	1.8	1.3
6	$O_{W1}-H_{13}$	−16.6	−14.4							−41.0	−17.0
7	$O_{W3}-H_{14}$	**1.3**	**1.1**	**0.6**	***0.6***	***0.7***	***0.6***				
8	$O_{W4}-H_5$									−9.0	−8.2
9	$O_{W6}-H_{13}$			1.3	1.6	1.4	1.2	0.8	0.6		
10	$O_{W6}-H_{10}$									−12.1	1.2

Charge = −2, $E^{(e)} \times 10^3$ (hartree/a_o^3)

		shift										
no.	bond	0	0.1 Å	0.2 Å	0.3 Å	0.4 Å	0.5 Å	0.6 Å	0.7 Å	0.8 Å	0.9 Å	1.0 Å
1	$^1O_{C1}-H_1$	−28	−322	−407	−476	−527	−551	−562	−4	−7	1	
2	$^2O_{C1}-H_2$											0
3	$^1O_{C2}-H_3$	1	0	0	0	0	0	0	−513	−537		−4
4	$^1O_{C2}-H_4$										0	
5	$^1O_{C2}-H_5$	−12		**1**	**1**	1	1	**1**				
6	$^2O_{C2}-H_5$		−4	1	**1**	**1**	***1***					
7	$O_{C3}-H_4$	3	3	3	3	3	2	2	0			1
8	$^1O_{C4}-H_6$									***1***		
9	$^1O_{C4}-H_7$										1	2
10	$^1O_{C4}-H_2$	−25	−4	−4	−2	0	1	1				
11	$^2O_{C4}-H_7$								−458	1		
12	$O_{W1}-H_5$										−654	
13	$O_{W1}-H_1$											−57
14	$O_{W2}-H_8$										−11	
15	$O_{W2}-H_5$								−626	−615		−4
16	$O_{W3}-H_9$	***1***	***1***	***1***								
17	$O_{W4}-H_2$										0	
18	$O_{W5}-H_8$	−7	−10	−5	−3	−1	1	1	−599	−3		
19	$O_{W5}-H_4$									**1**		
20	$O_{W5}-H_6$	−12	2	1	1	2	2	2			−10	−22
21	$O_{W6}-H_3$										1	
22	$O_{W6}-H_2$								1	2		

[a] See footnote *a* in Table 2.

as much as 2 orders of magnitude. If a bond does not disappear, the nature of the bond can change; its energy, its charge density, and all other properties suggest that the bonding is completely different after a transition than it is before.

Figure 7 shows a relation between the ellipticity and the bond length.

Discussion

Two results are of principal interest here: We have shown that there can be a large-scale transition of water molecules in a hydrogen bonded system with only a very limited motion of acid groups that define the boundary of the system. Second, hydrogen bonds in all the various forms of the system have properties that appear to belong to a single continuum; if this result turns out to be general, at least for O−H hydrogen bonds, it will have consequences for our understanding of hydrogen bonding, for the simulation of hydrogen bonds, and for conformational changes that involve these hydrogen bonds.

For the case of total charge = −2, the system shows at least two major minima in its potential energy surface, and one major conformational change. For total charge −1, we have two minima also, but also two changes in conformation. The two minima exist for a single position of the acetic acid moieties that determine the fixed part of the system. Optimization of the water coordinates and ionizable hydrogens, using standard criteria for convergence, can leave the system in either minimum, depending on the initial positions. We have not attempted to use more stringent criteria for convergence, as the main interest of the calculation is in determining the set of states that are easily accessible; if the behavior at 0 K were the only matter of interest, it would make sense to use criteria stringent enough to yield only the true global minimum. By obtaining two minima, it becomes possible to understand what may happen in an actual system. It also suggests the use of great caution in an MD simulation, as the path followed by the majority, probably very large majority, of trajectories may be determined by which minimum's basin happens to contain the starting configuration. Two minima can be included only by forcing the trajectories to sample both. In addition, the potentials used in the simulation would be unlikely to match the actual potentials; those found in the quantum mechanical calculation are approximately realistic, and cannot be easily represented by a function that fails to take into account the bond length effect that this calculation demonstrates. The calculations show that the potential for the interaction of a noncovalently bonded hydrogen and oxygen is strongly dependent on the surroundings. This does not rule out a potential that is suitably parametrized for the bond length effect; conceivably one parameter might suffice. Further work is needed to determine whether angular dependence matters, although we have no evidence of it as yet.

MD simulations in principle could use umbrella sampling around each of the minima. However, it is still not possible,

TABLE 4: Laplacian of Breaking OH Bonds[a]

$L = -{}^1/_4\nabla^2\rho \times 10^3\ (e/a_o{}^5)$, Charge = −1

		shift									
no	bond	0	0.1 Å	0.2 Å	0.3 Å	0.4 Å	0.5 Å	0.6 Å	0.7 Å	0.8 Å	0.9 Å
1	$O_{C1}-H_{10}$			−21	−22	−25	−24	−29	−26		
2	$O_{C1}-H_{11}$	−29	−24								
3	$O_{C2}-H_{11}$			−9	−9	−13	−8	−15	−11	−24	−21
4	$O_{C2}-H_5$	−7	−4								
5	$O_{C4}-H_{12}$	−20	−19	−8	−7	−10	−7	−13	−8	−11	−8
6	$O_{W1}-H_{13}$	−38	−38							−35	−41
7	$O_{W3}-H_{14}$	**−8**	**−7**	**−4**	***−3***	***−4***	***−3***				
8	$O_{W4}-H_5$									−38	−37
9	$O_{W6}-H_{13}$			−18	−15	−10	−7	−4	−3		
10	$O_{W6}-H_{10}$									−41	−26

$L = -{}^1/_4\nabla^2\rho \times 10^3\ (e/a_o{}^5)$, Charge = −2

		shift										
no.	bond	0	0.1 Å	0.2 Å	0.3 Å	0.4 Å	0.5 Å	0.6 Å	0.7 Å	0.8 Å	0.9 Å	1.0 Å
1	$^1O_{C1}-H_1$	−39	237	331	406	463	490	502	−32	−34	−8	
2	$^2O_{C1}-H_2$											−23
3	$^1O_{C2}-H_3$	−26	−27	−28	−29	−28	−29	−29	445	474		−36
4	$^1O_{C2}-H_4$										−2	
5	$^1O_{C2}-H_5$	−31		**−11**	**−10**	−8	−6	**−4**				
6	$^2O_{C2}-H_5$		−28	−14	**−10**	**−8**	***−5***					
7	$O_{C3}-H_4$	−19	−18	−17	−16	−15	−13	−11	−2			−4
8	$^1O_{C4}-H_6$									***−2***		
9	$^1O_{C4}-H_7$										−24	−14
10	$^1O_{C4}-H_2$	−33	−29	−28	−26	−22	−20	−20				
11	$^2O_{C4}-H_7$								386	−12		
12	$O_{W1}-H_5$										588	
13	$O_{W1}-H_1$											−23
14	$O_{W2}-H_8$										−36	
15	$O_{W2}-H_5$								561	550		−34
16	$O_{W3}-H_9$	***−5***	***−5***	***−5***								
17	$O_{W4}-H_2$										−27	
18	$O_{W5}-H_8$	−34	−34	−31	−30	−28	−24	−17	534	−32		
19	$O_{W5}-H_4$									**−5**		
20	$O_{W5}-H_6$	−39	−17	−26	−25	−22	−20	−20			−36	−39
21	$O_{W6}-H_3$										−27	
22	$O_{W6}-H_2$								−5	−11		

[a] See footnote a for Table 2.

using the standard potentials, to know that the second minimum exists, until it has actually been found. Umbrella sampling cannot help where the locations of the most important conformations of the system, or the configurations corresponding to energy minima, are not known.

In one sense, what has happened is simple. When the acetic acids are too close to the center, only two water molecules fit into the nearly planar configuration. The acetic acids are drawn back stepwise, 0.1 Å at a time. When a critical threshold is crossed, an additional water molecule enters the ring from immediately outside, forming a new set of hydrogen bonds, some of which are short and strong. The surprise is that the jump is a critical transition covering a large distance for the water molecule (≈2 Å) for a very short distance (≤0.05 Å in at least one case, always ≤0.1 Å), for the acid moieties that effectively set the boundary conditions for the system. In earlier work with Cl^-, we found a 0.005 Å shift of the Cl^- sufficed for a large transition of a single hydrogen bond in the center of an H_5O_2 within the ring of Cl^-, in a similar system.[2] The transition is not gradual. We have related this to the electron density, to the bonding, and to related properties, including the ellipticity. The AIM ellipticity applies to one bond at a time, so the few large values predict changes in only that bond, but not in the system as a whole. There is a set of systemic changes that no single bond can represent. However, there is a relation between ellipticity and the bond length, so that it is a property of bonding consistent with the remainder of the analysis. Because the ellipticity is a bond-by-bond index, Tables 2−5 also show the pattern of bonding. Looking at these tables, even without considering the numbers, makes it immediately obvious where there has been a switch in the topology of the bonding of the system; the locations at which the series of values of ellipticity and other properties simply ends, and a new series begins, are clear from the pattern of blank spaces.

We can consider applying the results to protein conformational changes. Although we began with a hypothesis concerning ion channel gating,[1,34,45] the results of this work should be more general. It remains to be demonstrated that conformational changes that accompany enzyme catalysis are related to this phenomenon, but it is known that catalytic sites have more than the statistically expected number of ionizable residues[46] making it plausible that they form critical hydrogen bonds. It is reasonable to expect that transitions such as the one we are looking at here could occur as a part of the catalytic cycle in at least some cases. It is also known that many protein functions are pH dependent; the bonding pattern here is also quite different when the charge on the system changes, suggesting application of these ideas to pH dependent processes.

There is a continuum of hydrogen bonds, from weak and long to strong and short. The electron density at BCPs as defined by AIM decreases exponentially with bond length, and a single curve applies to the entire range of O−H bonds. The bond order

TABLE 5: Potential Energy Density of Breaking OH Bonds[a]

V $\times -10^3$ (hartree/a_o^3), Charge = −1

		shift									
no.	bond	0	0.1 Å	0.2 Å	0.3 Å	0.4 Å	0.5 Å	0.6 Å	0.7 Å	0.8 Å	0.9 Å
1	$O_{C1}-H_{10}$			17	19	23	21	28	24		
2	$O_{C1}-H_{11}$	26	20								
3	$O_{C2}-H_{11}$			6	6	9	5	10	7	21	17
4	$O_{C2}-H_5$	5	3								
5	$O_{C4}-H_{12}$	14	13	6	5	7	5	9	6	8	6
6	$O_{W1}-H_{13}$	72	67							117	75
7	$O_{W3}-H_{14}$	**6**	**5**	**2**	***2***	***3***	***2***				
8	$O_{W4}-H_5$									56	54
9	$O_{W6}-H_{13}$			16	12	7	5	3	2		
10	$O_{W6}-H_{10}$									65	23

V $\times -10^3$ (hartree/a_o^3), Charge = −2

		shift										
no.	bond	0	0.1 Å	0.2 Å	0.3 Å	0.4 Å	0.5 Å	0.6 Å	0.7 Å	0.8 Å	0.9 Å	1.0 Å
1	$^1O_{C1}-H_1$	95	406	484	546	591	613	623	40	49	6	
2	$^2O_{C1}-H_2$											23
3	$^1O_{C2}-H_3$	24	26	28	28	28	28	28	581	601		44
4	$^1O_{C2}-H_4$										1	
5	$^1O_{C2}-H_5$	56		**9**	**8**	6	4	**3**				
6	$^2O_{C2}-H_5$		37	11	**8**	**5**	***4***					
7	$O_{C3}-H_4$	13	12	11	10	10	8	7	1			2
8	$^1O_{C4}-H_6$									***1***		
9	$^1O_{C4}-H_7$										23	9
10	$^1O_{C4}-H_2$	82	37	37	30	23	19	19				
11	$^2O_{C4}-H_7$								530	9		
12	$O_{W1}-H_5$										720	
13	$O_{W1}-H_1$											137
14	$O_{W2}-H_8$										58	
15	$O_{W2}-H_5$								691	681		43
16	$O_{W3}-H_9$	***4***	***3***	***3***								
17	$O_{W4}-H_2$										28	
18	$O_{W5}-H_8$	48	55	41	35	30	23	14	665	39		
19	$O_{W5}-H_4$									**3**		
20	$O_{W5}-H_6$	63	13	24	22	18	16	16			55	84
21	$O_{W6}-H_3$										25	
22	$O_{W6}-H_2$								3	7		

[a] See footnote *a* for Table 2.

is strongly correlated with the AIM properties. To understand the behavior of the system it is necessary, however, to consider much more than one bond at a time. In the example we have here, several water molecules move, and one or two move a great deal, at the transition point. There is no possibility therefore of looking at the density in this system and finding a single change of density that explains the entire transition. The bonding switches in several places to produce the new configuration. Sometimes not all the switches occur simultaneously, which results in apparent hysteresis. Bond topology is a system property and not the property of individual bonds.

The Zundel ion, $H_5O_2^+$, when isolated, is symmetric, with two O−H distances of 1.2 Å.[47] When surrounding molecules are added, this symmetry is destroyed. We observed in our earlier work[1,2] that the more symmetric central hydrogen bond was found when the surrounding groups were moved to a greater distance from the central bond, presumably making the effect of the surrounding group weaker, as expected from the vacuum result for the Zundel ion cited above. With the covalent and hydrogen bonds apparently belonging to the same continuum with respect to several properties in AIM, it may not make sense to regard SSHB as qualitatively different from either the covalent bonds or the ordinary hydrogen bonds, but as intermediate parts of a continuum.

It would be extremely useful for there to be some form of experimental test for these ideas. This is not easy. There are some hints from existing data. We have noted that changing charge is another way to change the topology of hydrogen bonds in a complex system; changing pH should have this effect. One system that shows an extremely strong pH dependence, possibly a sudden change, may be an example of the kind of effect we are discussing.[36,37] This system, the OmpF pore of *Escherichia coli*, has a constriction of about 7 Å × 11 Å, roughly similar to what we have here. There are several residues that can be charged, and their charge state may change with pH. However, by itself, the difference in charge, and the electric field, do not appear able to alter the permeability with anything like the steepness that is found, about 7-fold in channel blockage over half a pH unit. An attempt to explain the effect has been made by Mafe et al.,[48] but this still does not appear to suffice. A sharp transition in the topology of the hydrogen bonds of the system would be consistent with the results. Further work would be required to confirm this, starting from the structure of the channel. The original system for which our calculation was begun, the KcsA channel, has since been shown to have different coordinates,[49] so that it may not be so easy to use it as a test; it still gates with pH, of course, but we have a different, albeit related, model of how that occurs with the new coordinates.

The calculation is effectively at 0 K. At 300 K, there will be averaging of the positions over the two sets of minima, unless the difference in energy is appreciably larger than it is here over most of the range. In calculating the thermodynamic properties of the system, this is important. However the fact that there are two sets of minima is not affected by the finite temperature. In

an MD simulation, it would be necessary to ensure that paths including both minima were included at the simulation temperature, as the averaged properties of the system would clearly include both. Therefore, to do an MD study of a system with hydrogen bonds that could have two minima, two possibilities exist: a QM/MM method that would give the two minima could be used (there are several methods that might), or else the potential energy surface (PES) could be determined first, followed by a simulation in which an umbrella potential or some other method were used to ensure that trajectories covering both minima were appropriately included. Once the existence of the two minima is confirmed, the rest of the PES might be determined by one of two methods: (1) by finding a transition state and then looking in the neighborhood of the transition state with a Monte Carlo simulation of points on the path near the transition state or (2) by trying points on a path between minima, and then points in the immediate vicinity of the points on the path. We are studying the possibilities at present.

Conclusions

Hydrogen bonds of O−H−O type appear to form a continuum in their bonding properties, over the entire range of length and strength of hydrogen bonds. Some properties even show the covalent OH bonds as falling on the same curves as the hydrogen bonds.

At certain critical points in the geometry of the system, a catastrophic rearrangement of the hydrogen bonding of the system can occur, leading to a very different topology of the hydrogen bonds, and of the position of water molecules, in the system.

As a consequence of the second conclusion, molecular dynamics simulations are likely to need to be adjusted to allow for these discontinuous effects.

Acknowledgment. This work has been supported in part by an NIH SCORE grant (through CCNY) and a PSC/CUNY grant. We are also grateful to the reviewers for a very detailed reading of the manuscript, with helpful comments.

References and Notes

(1) Green, M. E. *J. Phys. Chem. B* **2001**, *105*, 5298.
(2) Green, M. E. *J. Phys. Chem. A* **2002**, *106*, 11221.
(3) Grabowski, S. J. *J. Phys. Chem. A* **2001**, *105*, 10739.
(4) Bader, R. F. W. *Atoms in Molecules: A Quantum Theory*; Oxford, U. P.: Oxford, England, 1990.
(5) Popelier, P. *Atoms in Molecules, An Introduction*; Prentice Hall/Pearson Education: Harlow, England, 2000.
(6) Biegler-Konig, F.; Schoenbohm, J. *AIM2000*, 2.0 ed.; Buro fur Innovative Software: Bielefeld, Germany, 2002.
(7) Weinhold, F. *NBO 5.0 Program Manual*; Theoretical Chemistry Institute, University of Wisconsin: Madison, WI 2001.
(8) DuPre, D. B. *J. Phys. Chem. A* 2003.
(9) Mallinson, P. R.; Smith, G. T.; Wilson, C. C.; Grech, E.; Wozniak, K. *J. Am. Chem. Soc.* **2003**, *125*, 4259.
(10) Bartlett, G. J.; Porter, C. T.; Borkakoti, N.; Thornton, J. M. *J. Mol. Biol.* **2002**, *324*, 105.
(11) Lin, K.-J.; Cheng, M.-C.; Wang, Y. *J. Phys. Chem.* **1994**, *98*, 11685.
(12) Adam, K. R. *J. Phys. Chem. A* **2002**, *106*, 11963.
(13) Kobko, N.; Dannenberg, J. J. *J. Phys. Chem. A* **2003**, *107*, 10389.
(14) Lipkowski, P.; Koll, A.; Karpfen, A.; Wolschann, P. *Chem. Phys. Lett.* **2002**, *360*, 256.
(15) Mautner, M. M. N.; Elmore, D. E.; Scheiner, S. *J. Am. Chem. Soc.* **1999**, *121*, 7625.
(16) Lefohn, A. E.; Ovchinnikov, M.; Voth, G. A. *J. Phys. Chem. B* **2001**, *105*, 6628.
(17) Schmitt, U. W.; Voth, G. A. *Isr. J. Chem.* **1999**, *39*, 483.
(18) Lu, D.; Voth, G. A. *J. Am. Chem. Soc.* **1998**, *120*, 4006.
(19) Schmitt, U. W.; Voth, G. A. *J. Phys. Chem. B* **1998**, *102*, 5547.
(20) Lobaugh, J.; Voth, G. A. *J. Chem. Phys.* **1996**, *104*, 2056.
(21) Day, T. J. F.; Soudackov, A. V.; Cuma, M.; Schmitt, U. W.; Voth, G. A. *J. Chem. Phys.* **2002**, *117*, 5839.
(22) Billeter, S. R.; Webb, S. P.; Iordanov, T.; Agarwal, P. K.; Hammes-Schiffer, S. *J. Chem. Phys.* **2001**, *114*, 6925.
(23) Hammes-Schiffer, S. *Biochemistry* **2002**, *41*, 13335.
(24) Kim, S. Y.; Hammes-Schiffer, S. *J. Chem. Phys.* **2003**, *119*, 4389.
(25) Krasnoholovets, V. V.; Tomchuk, P. M.; Lukyanets, S. P. *Adv. Chem. Phys.* **2003**, *125*, 351.
(26) Garcia-Viloca, M.; Gao, J.; Karplus, M.; Truhlar, D. G. *Science* **2004**, *303*, 186.
(27) Cleland, W. W. *Arch. Biochem. Biophys.* **2000**, *382*, 1.
(28) Lin, J.; Frey, P. A. *J. Am. Chem. Soc.* **2000**, *122*, 11258.
(29) Cleland, W. W.; Frey, P. A.; Gerlt, J. A. *J. Biol. Chem.* **1998**, *273*, 25529.
(30) Frey, P. A.; Cleland, W. W. *Bioorg. Chem.* **1998**, *26*, 175.
(31) Kim, K. S.; Kim, D.; Lee, J. Y.; Tarakeshwar, P.; Oh, K. S. *Biochemistry* **2002**, *41*, 5300.
(32) Kim, K. S. O.; K. S.; Lee, J. Y. *Proc. Natl Acad. Sci. U.S.A.* **2000**, *97*, 6373.
(33) Doyle, D. A.; Cabral, J. M.; Pfuetzner, R. A.; Kuo, A.; Gulbis, J. M.; Cohen, S. L.; Chait, B. T.; MacKinnon, R. *Science* **1998**, *280*, 69.
(34) Green, M. E. *J. Biomol. Struct. Dynamics* **2002**, *19*, 725.
(35) Green, M. E. *Biophys. J.* **2001**, *80*, A837.
(36) Nestorovich, E. M.; Rostostseva, T. K.; Bezrukov, S. M. *Biophys. J.* **2003**, *85*, 3718.
(37) Nestorovich, E. M.; Danelon, C.; Winterhalter, M.; Bezrukov, S. M. *Proc. Natl Acad. Sci. U.S.A.* **2002**, *99*, 9789.
(38) Frisch, M. J.; Trucks, G. W.; Schlegel, H. B.; Scuseria, G. E.; Robb, M. A.; Cheeseman, J. R.; Montgomery, J. A., Jr.; Vreven, T.; Kudin, K. N.; Burant, J. C.; Millam, J. M.; Iyengar, S. S.; Tomasi, J.; Barone, V.; Mennucci, B.; Cossi, M.; Scalmani, G.; Rega, N.; Petersson, G. A.; Nakatsuji, H.; Hada, M.; Ehara, M.; Toyota, K.; Fukuda, R.; Hasegawa, J.; Ishida, M.; Nakajima, T.; Honda, Y.; Kitao, O.; Nakai, H.; Klene, M.; Li, X.; Knox, J. E.; Hratchian, H. P.; Cross, J. B.; Adamo, C.; Jaramillo, J.; Gomperts, R.; Stratmann, R. E.; Yazyev, O.; Austin, A. J.; Cammi, R.; Pomelli, C.; Ochterski, J. W.; Ayala, P. Y.; Morokuma, K.; Voth, G. A.; Salvador, P.; Dannenberg, J. J.; Zakrzewski, V. G.; Dapprich, S.; Daniels, A. D.; Strain, M. C.; Farkas, O.; Malick, D. K.; Rabuck, A. D.; Raghavachari, K.; Foresman, J. B.; Ortiz, J. V.; Cui, Q.; Baboul, A. G.; Clifford, S.; Cioslowski, J.; Stefanov, B. B.; Liu, G.; Liashenko, A.; Piskorz, P.; Komaromi, I.; Martin, R. L.; Fox, D. J.; Keith, T.; Al-Laham, M. A.; Peng, C. Y.; Nanayakkara, A.; Challacombe, M.; Gill, P. M. W.; Johnson, B.; Chen, W.; Wong, M. W.; Gonzalez, C.; Pople, J. A. *Gaussian 03*, revision B.03; Gaussian, Inc.: Pittsburgh, PA, 2003.
(39) Laaksonen, A. *J. Mol. Graph.* **1992**, *10*, 33.
(40) Becke, A. D. *J. Chem. Phys.* **1996**, *104*, 1040.
(41) Becke, A. D. *Phys. Rev. A* **1988**, *38*, 3098.
(42) Krishnan, R.; Binkley, J. S.; Seeger, R.; Pople, J. A. *J. Chem. Phys.* **1980**, *72*, 650.
(43) Arnold, W. D.; Oldfield, E. *J. Am. Chem. Soc.* **2000**, *122*, 12835.
(44) Pacios, L. F. *J. Phys. Chem. A* **2004**, *108*, 1177.
(45) Sapronova, A. V.; Bystrov, V. S.; Green, M. E. *Frontiers Biosci.* **2003**, *8*, s1356.
(46) Gu, Z.; Zambrano, R.; McDermott, A. *J. Am. Chem. Soc.* **1994**, *116*, 6368.
(47) Xie, Y.; Remington, R. B.; Schaefer, H. F. *J. Chem. Phys.* **1994**, *101*, 4878.
(48) Mafe, S.; Garcia-Morales, V.; Ramirez, P. *Chem. Phys.* **2003**, *296*, 29.
(49) Zhou, Y.; Morais-Cabral, J. H.; MacKinnon, R. *Nature (London)* **2001**, *414*, 43.